LA-UR- 07- 1597

Approved for public release; distribution is unlimited.

Title: DEVELOPMENT OF AN INTEGRATED SOFTWARE SOLUTION FOR PIEZOELECTRIC ACTIVE-SENSING IN STRUCTURAL HEALTH MONITORING

Author(s): Laura D. Jacobs, LANL, INST-OFF
GyuHae (NMI) Park, LANL, INST-OFF
Charles R. Farrar, LANL, INST-OFF

Submitted to: SPIE INTERNATIONAL SYMPOSIUM ON SMART STRUCTURES AND NONDESTRUCTIVE EVALUATION,SAN DIEGO, CA, MAR. 18-22, 2007.

Los Alamos
NATIONAL LABORATORY

Development of an Integrated Software Solution for Piezoelectric Active-Sensing in Structural Health Monitoring

Laura D. Jacobs[1], Gyuhae Park[2], Charles R. Farrar[2]
[1]Department of Civil and Environmental Engineering, Georgia Institute of Technology, Atlanta, GA 30332
[2]Engineering Institute, MS T001, Los Alamos National Laboratory, Los Alamos, NM 87545

ABSTRACT

In this study, a novel approach of integrating data interrogation algorithms of active sensing methods for structural health monitoring (SHM) applications, including Lamb wave propagation, impedance method, and sensor-diagnostics, is presented. Contrary to most active-sensing SHM techniques, which utilize only a single signal processing method for damage identification, a suite of signal processing algorithms are employed and grouped into one package to improve the damage detection capability. A MatLab-based user interface called H.O.P.S. (Health Of Plate Structures) was created, which allows the analyst to configure the data acquisition system and display the results from each damage identification algorithm for side-by-side comparison. This side-by-side comparison of results simplifies the task of identifying the relative effectiveness and sensitivity of each algorithm. By grouping a suite of algorithms into one package, this study contributes to and enhances the visibility and interpretation of the active-sensing methods related to damage identification in a structure.

1. INTRODUCTION

Structural health monitoring (SHM) is the process of measuring the dynamic response of a structure and determining the current state of the structure's health. The process is typically done by comparing the signal from the current, potentially damaged, system to a database of signals collected from the structure in a known healthy state. The advantages of SHM include the detection of incipient damage, before it becomes extensive and potentially cause catastrophic failure. In this paper, a comprehensive SHM software solution based on guided wave and impedance-based techniques is developed. Some of the guided wave techniques in this software are based of the work performed by Swartz, et al.[12], Lee and Staszewski6 Kessler, et al.[7], and Sohn et al[9]. The impedance method is based on the work performed by Park, et al.[1, 11], Giurgiutiu et al. [12], and Bhalla et al. [13], and sensor diagnostics and validation process on Park et al [5,15]

In this study a MatLab-based graphical user interface called H.O.P.S. (Health of Plate Structures) was created to allow the analyst to configure a data acquisition system and display the results in a side-by-side comparison. This side-by-side comparison simplifies the task of identifying the relative effectiveness and sensitivity of each active-sensing method and algorithm. The grouping of a suite of algorithms into a single package enhances the visibility and interpretation of the active-sensing methods related to damage identification. The first technique is for diagnostics and validation of the sensors. Sensor diagnostics is a critical step in the SHM process, because it is important to identify if the change in readings is caused by a damaged sensor, or damage within the structure itself. The second damage identification technique involves the comparison of impedance measurements. The third set of damage identification techniques use measurements from guided waves, which include: a comparison of wave attenuation in an undamaged plate and a damaged plate; the cross-correlation coefficient of the power spectral densities of the baseline and test signals; the identification of waves reflected off of the damage. More detailed descriptions of the damage identification techniques can be found in next sections.

2. H.O.P.S. SIGNAL PROCESSING ALGORITHMS

Three main categories of structural health monitoring techniques are utilized in H.O.P.S.: sensor diagnostics, impedance-based analysis, and a guided wave base technique. The algorithms used for signal processing were written

as MatLab functions and integrated by the use of a MatLab GUI. H.O.P.S. program is also designed to communicate with the data acquisition system directly. For the case the hardware is not supported by H.O.P.S., the data collected could be imported into H.O.P.S. using the Data Import function.

2.1 Sensor Diagnostics

The principle of sensor self-diagnostics is to track the changes in the imaginary portion of the electrical admittance, which is analogous to the capacitive value, of the piezoelectric (PZT) material.[5] The imaginary portion of the electrical admittance is a function of the geometry constants and the mechanical and electrical properties of a PZT transducer. Changes in any of these properties are manifested in the imaginary portion of the electrical admittance. Thus, breaking of the sensor and the subsequent degradation the sensor parameters can be identified by monitoring the imaginary portion of the electrical admittance.. Breaking of the sensor causes a downward shift in the slope of the admittance, i.e. decrease in the capacitance, because the effective size of the sensor decreases. It is also possible to identify changes in the bonding conditions of the PZT transducer. As the transducer becomes debonded, it causes an upward shift in the slope of the admittance, which indicates the increase in the capacitance. Therefore, by monitoring the slope of the imaginary part of the admittance for a PZT transducer, one can obtain the information about the functionality of the transducer. A more detailed description on the sensor diagnostic process can be found in the reference.[5, 15]

The sensor diagnostics are performed in two different ways in H.O.P.S.. The first is making a comparison of the readings from all of the sensors with each other; so only one set of readings from each sensor is needed. The second technique is to compare multiple readings from each sensor with the baseline readings from that sensor. In both techniques, to make a comparison of the slope of the admittance curve, the area under the curve is calculated using the trapezoidal rule. When only one set of data is being compared, the average and standard deviation of the areas are determined. A plot of the area under the admittance curve vs. sensor is plotted to aid the user in selecting a cutoff for when a sensor has debonded or is broken. Once the cutoffs have been specified, a plot of the plate is displayed with the broken sensors in magenta and the debonded sensors in blue. When multiple data sets are being compared, two plots are displayed: admittance vs. sensor and admittance vs. temperature. These plots assist the user in determining how temperature affects the admittance measurements and to aid in the selection of the cutoff values that reflect damage rather than temperature changes. Once the cutoffs have been selected, a plot of the plate, similar to the one created for the single data set sensor diagnostics, is displayed.

2.2 Impedance method

Impedance based structural health monitoring methods use high-frequency structural excitations, typically higher than 30 kHz, through surface bonded piezoelectric patches to monitor changes in structural mechanical impedance [1]. The electrical impedance is a function of the mechanical impedances of the PZT actuator and the host structure. Assuming that the mechanical impedance of the PZT does not change over time, any changes in the electrical impedance measurement can be considered an indication of a change in the mechanical impedance of the host structure. A change in the mechanical impedance of the host structure is due to damage. The change in impedance due to damage is exhibited only in the real portion of the impedance signature.[1]

A quantitative assessment of damage is traditionally made using a scalar damage metric[1], which is adopted in H.O.P.S.. Two simple statistical algorithms can be used to yield a damage metric. The first is to find the cross-correlation coefficient between the baseline and test signals. The cross-correlation coefficient between the two data sets determines the relationship between the two signals. The cross-correlation coefficient is subtracted from one yielding a damage index between 0 and 1, where larger values indicate a greater extent of damage. This damage index is relatively insensitive to temperature. The second method is based on a frequency-by-frequency comparison and is referred to as the root-mean-square-deviation (RMSD), and is defined as:

$$M = \sum_{i=1}^{n} \sqrt{\frac{[\mathrm{Re}(Z_{i,1}) - \mathrm{Re}(Z_{i,2})]^2}{[\mathrm{Re}(Z_{i,1})]^2}} \tag{1}$$

where M is the damage metric, $Z_{i,1}$ is the impedance of the baseline measurement, and $Z_{i,2}$ is the test measurement at frequency interval I.[1] This method is sensitive to temperature effects, so some normalization of the signal is usually necessary.

Temperature greatly affects the impedance measured at each frequency due to the effects of temperature on the dielectric constant of the PZT and the modulus of elasticity of the structure.[11] The primary effects of changing temperature are to shift the real part of the impedance with respect to the frequency and to shift the amplitudes. To counter this effect, Park et al.[11] proposed replacing the real part of the impedance in Equation 1 with the following:

$$\mathrm{Re}(Y_{j,2}) = \mathrm{Re}(Y_{j,2})_{measured} + \delta^{s} \tag{2}$$

where $\mathrm{Re}(Y_{j,2})$ is the real part of the impedance of the test signal, δ_S is defined as the average difference between the baseline impedance and the test impedance. By this equation, the vertical and horizontal shifts of the impedance signature caused by environmental condition changes are minimized. The coefficients are iterated, searching for the minimum value of the damage metric. Because changes in the structural properties due to damage change the shape of the impedance curve drastically, Park et al's proposed normalization process will result in a large damage metric for changes due to structural damage and a negligible damage metric for changes in temperature.[11]

2.3 Guided Wave

As guided wave-based SHM methods look for the possibility of damage using many different features, such as wave attenuation, wave signal distortion, and reflection, three different signal processing methods are employed in H.O.P.S.

2.3.1 Wave Attenuation

As Lamb waves propagate through a structure, the mechanical energy is dissipated, causing a decrease in the magnitude of the wave. The amount of attenuation between two points on a structure changes when damage is located in the path between them. By comparing the amplitude of the packets in a baseline measurement to those in a test measurement, conclusions can be made about the existence of damage between the actuator and sensor. Often the sensors will measure additional packets, which are reflections of the Lamb wave off of the edge of the plate. The amplitude of the reflections can be used to identify the existence of damage, but it can be difficult to determine the location of the damage. When using this approach to identify the existence of damage, care must be taken to ensure the packet of interest contains a wave that travels directly from the actuator to the sensor. To achieve an attenuation comparison between a baseline measurement and a test measurement, both signals are transformed using a wavelet transformation in H.O.P.S. An accurate wavelet transform is achieved by using a basis function that is the same as the input function.[8, 10] The wavelet transform is:

$$Wf(u,s) = \int_{-\infty}^{\infty} f(t)\frac{1}{\sqrt{s}}\Psi^{*}_{u,s}(t)dt \tag{3}$$

where u refers to the translations and s refers to the dilations of the mother wavelet, which is defined as:

$$\Psi^{*}_{u,s} = \frac{1}{\sqrt{s}}\psi\left(\frac{(t-u)}{s}\right). \tag{4}$$

A damage index (DI) can be calculated based on a ratio of the kinetic energy of the test signal to that of the baseline, as in Equation 3. The damage index is based on that of Swartz et al.[12].

$$DI = \left| \frac{\int_{u0}^{u1} Wf_{t}(u,s_0)du - \int_{u0}^{u1} Wf_{b}(u,s_0)du}{\int_{u0}^{u1} Wf_{b}(u,s_0)du} \right| \tag{5}$$

In Equation 4, the t represents the test signal and b represents the baseline signal, u_0 and u_1 represent the starting and ending time points for the S_0 mode. The DI ranges from 0, no damage, to a maximum value of 1 as the attenuation increases. A more detailed description of the technique can be found in Sohn, et al..[9]

Once the damaged paths have been determined, they are plotted on a predefined grid. The number of damaged paths intersecting at each grid point is divided by the number of undamaged paths intersecting at that point. The result is then normalized over the entire grid. The normalized values are plotted on a grid in the H.O.P.S. user interface to indicate the most likely locations of damage.[12]

2.3.2 Power Spectral Density

A second method of feature extraction for the Lamb wave data involves the cross-correlation of the power spectral density functions between the baseline and test signals. When a wave passes through damage, such as corrosion or a crack, the wave is scattered, referred to as mode conversion, causing a change in the frequency content of the signal. By looking at the amount of frequency content change, one can determine that the path contains structural damage. After measuring the propagated wave, the power spectral density (PSD) is calculated at the excitation frequency for the baseline and test signals. As in the work by Swartz et al.,[12] the damage index is based on the cross-correlation coefficient of the two PSDs, which identify the shape changes in PSD curves, and hence, identify the frequency content distortion. For consistency with the other feature extraction methods, the cross-correlation coefficient is subtracted from one, so that the signals with the highest correlation (the lowest amount of damage) have a damage index very close to zero, while signals with low correlation (high amounts of damage) have a higher damage index.

2.3.3 Triangulation of Reflected Waves

When Lamb waves travel through damage, some of the waves reflect off of the damage, creating new wave arrivals in the received signal. The third method of feature extraction for Lamb waves uses the reflection features to locate the damage.

In H.O.P.S., a wavelet transform is first performed on the signal to remove noise. Then, the arrival time for the first wave is calculated for each path. The distances for the paths are calculated by using the x and y coordinates of the sensors involved. The arrival time and distances are used to calculate the wave speed. The wave speeds are averaged to approximate the wave speed of the plate. Then, a Hilbert transform is performed on the signals, so that only an envelope of the signal remains and a slight phase shift of baseline and test signals can be removed. The envelope of tThe baseline signal is then subtracted from that of the test signal, thereby identifying new reflected waves. Once the first two new reflected waves are identified for every path, and the distances they traveled are calculated. An ellipse is then drawn around the two sensors, where the line of the ellipse is the distance from the two sensors where the damage could be located. Then, all of the places where ellipses cross are found and recorded. A graph of the plate is then drawn with X's located where the ellipses crossed. The ellipses can cross in multiple locations, so the user must determine where the most X's are located, the area of which most likely contain the damage.

3. H.O.P.S. SOFTWARE

H.O.P.S. user graphical interface is created to merge the various SHM signal processing method described in the previous section, as shown in Figure 1. Included also in H.O.P.S. is the geometry module that configures the structural parameters and the sensor/actuator configuration, and the data import module that can transport data for being processed in H.O.P.S. (for hardware that are not currently supported by this software). This program is also designed in such a way that the measured data and the hardware parameters can be dynamically saved and loaded for the future analyses. Each of the five buttons displayed in Figure 1 opens one of the modules of H.O.P.S.. The five modules are: Geometry, Import Data, Impedance, Wave Propagation and Sensor Diagnostics. Data and variables are

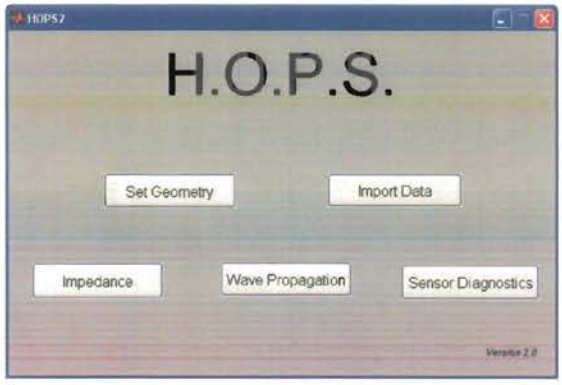

Figure 1: H.O.P.S. Main Function GUI

passed between modules through this main function. By integrating hardware and several signal processing algorithms into one package, H.O.P.S. can be an efficient SHM tool for various applications, allowing the uses to select the most suitable algorithm for different forms of damage in different applications.

4. EXPERIMENTAL SETUP AND PROCEDURES

The experiments are performed to investigate the performance of H.O.P.S.. The test structure is an aluminum plate instrumented with an array of PZT transducers. The sensor diagnostics process is first carried out in order to assess the sensor installation condition. Damage to the structure is introduced in the form of corrosion, which is the most typical type of damage in aluminum plates. Guided wave and impedance measurements are then taken before and after the damage to assess the condition of the plate. All the signal processing process is performed using H.O.P.S. and only selected results are presented due to the space constraints of the paper.

4.1 Setup and Procedure

The aluminum plate used in this study had the dimensions of 1219 mm (4 feet) square. The plate was instrumented with two arrays of nine PZT transducers. The transducers were spaced at 304.8 mm (12 inches) (Figure 2). One side of the plate had 6.35 mm (0.250 inches) diameter circular PZT transducers. The other side had 12.7 mm (0.500 inches) diameter circular PZT transducers. The PZT transducers were bonded to the plate using a quick-setting adhesive. The transducers were numbered 1 to 9 in the grid as shown in Figure 3. The Lamb wave data are acquired using a commercial system capable of sampling up to 25 MHz. The impedance and sensor diagnostic data are collected with an Agilent impedance analyzer.

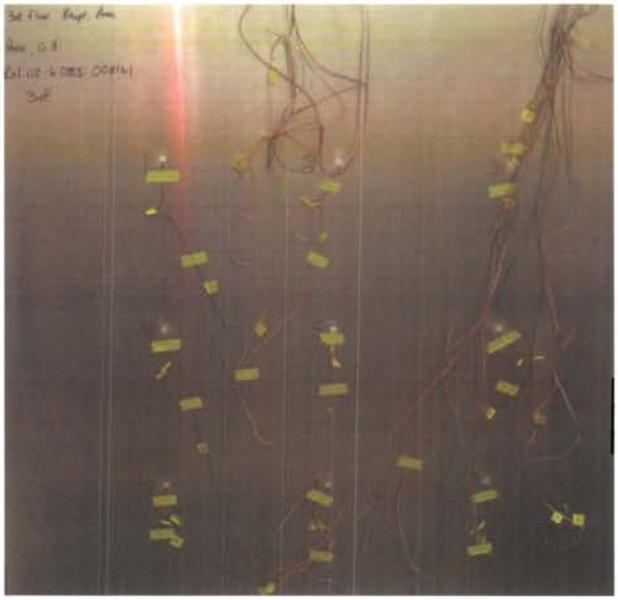

Figure 2: Experimental Plate

To simulate damage in a reversible manner, putty is first affixed to the plate in sizes ranging from one to 3 inches in diameter, which adds mass and damping to the certain area of the structure. The putty provided a removable damage case that could be moved to any location on the plate in order to test the H.O.P.S signal processing algorithm without creating permanent damage to the structure. The putty is placed in various locations on the plate. Multiple damage locations are also simulated by affixing two pieces of putty in different locations on the plate. Irreversible damage is then introduced in the form of corrosion. A mixture of water and table salt, an aluminum cathode and a power supply are used to introduce corrosion. Measurements are taken after each stage of the damaged conditions to gather information about how sensitive the signal processing algorithms were to the amount of corrosion.

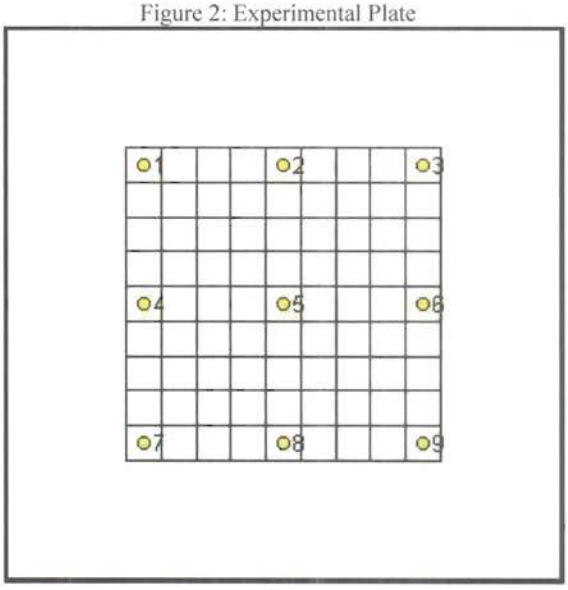

Figure 3: Sensor Numbering Scheme.

To perform a sensor diagnostics test, a frequency range of 1 - 20 kHz is used. The signal is collected by an impedance analyzer and then is imported into H.O.P.S. using the Data Import function. For an impedance test, the frequency range of interest is 185 kHz to 190 kHz. This range contains several peaks and does not contain the natural frequency of the PZT transducer, so it is a useful range for getting information about the health of the plate structure. The temperature was also recorded using a thermocouple attached to the plate. The

signal is recorded using an impedance analyzer and then imported into H.O.P.S..

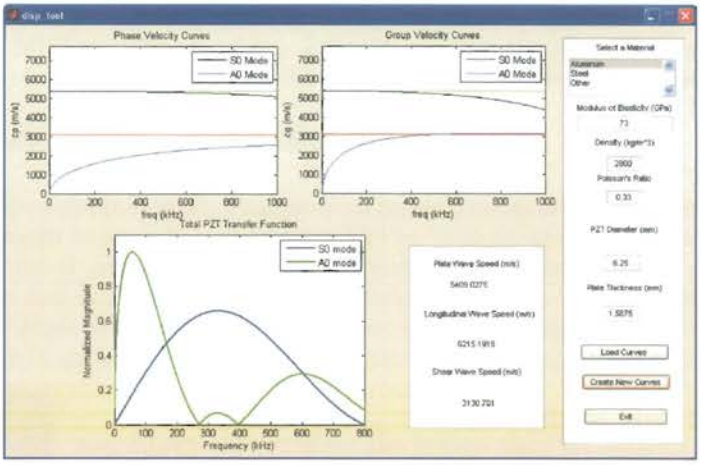

Figure 4: Dispersion curve and Transfer Function Tool.

Four different frequencies were used for the guided wave portion of the study. Table 1 summarizes the frequencies used in this study. The fundamental symmetric mode, or S_0 mode, is often used in SHM because it is the least dispersive and fastest of the waves. However, because of the non-dispersive nature and the long-wave length of the S_0 mode, it is insensitive to small defects in a structure. The fundamental anti-symmetric mode, or A_0 mode, is more dispersive than the S_0 mode, but is more sensitive to certain types of damage. The A_0 mode can be isolated from the other modes if the proper driving frequency is chosen. The driving frequencies for the various modes are dependent on the size of the PZT used. Included in H.O.P.S is a tool that creates the group and phase velocity of the plate and transfer function of PZT transducers that helps to select the desired driving frequency. Figure 4 shows the curves from the tool for a 1.59 mm (0.0625 inch) plate and 6.35 mm (0.25 inch) diameter transducers.

Table 1: Frequencies for S_0 and A_0 modes for various PZT sizes

	A_0	S_0
6.35 mm diameter PZT	80 kHz	300 kHz
12.7 mm diameter PZT	40 kHz	125kHz

5. RESULTS

The experimental results illustrate the performance of H.O.P.S. Each module and each signal processing techniques are utilized in order to provide the effectiveness of the software.

5.1 Geometry and Data Import

In H.O.P.S., The Geometry module allows the user to define the size and the shape of the structure, sensor locations, the size of a grid to be used for locating damage, and the sensor paths that can be used for the Wave Propagations. Data collected with programs other than H.O.P.S. can be imported using the Import Data module. The geometry and the automatically generated sensor paths defined for the test structure is shown in Figure 5.

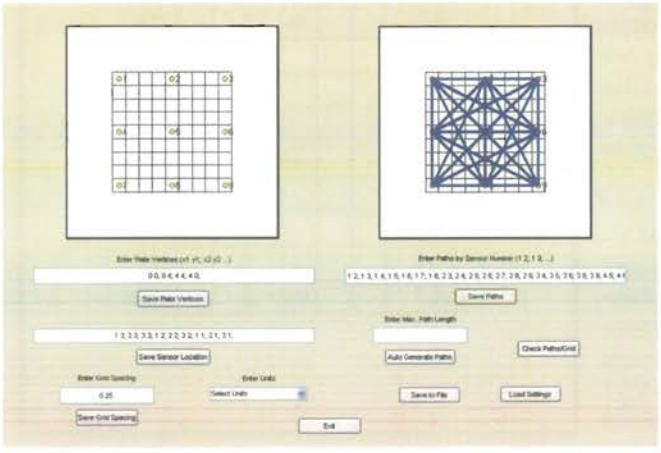

Figure 5: Geometry Module GUI

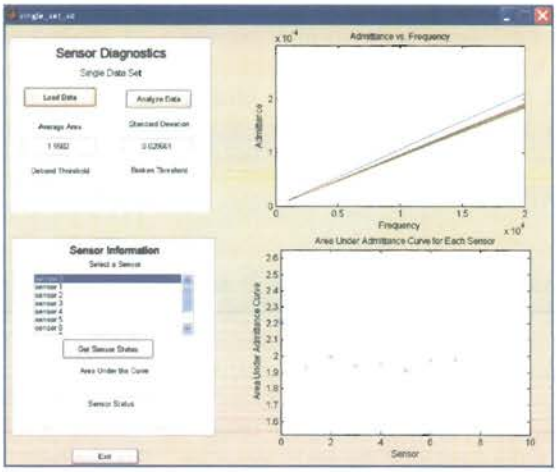

Figure 6: Sensor Diagnostics Data for 1/4" PZTs

5.2 Sensor diagnostics

Sensor diagnostics are then performed to confirm if all of the sensors are functioning properly and are all bonded to a similar level. As is shown in Figure 6, the quarter-inch PZTs in this study were bonded such that the average area under the admittance curves is 1.9582 and the standard deviation is 0.0297. These results indicate that the quarter-inch PZTs are bonded to a consistent level and none were broken or de-bonded in the bonding process. The user can set the threshold limit for sensor damage identification dynamically by looking at the statistics values in conjugation with the graph provided. In such a way, misclassification (false-positive or false-negative) can be reduced.

5.3 Impedance analysis

H.O.P.S. is also designed to store the measurement history into a database, so that one can track the variation of signatures, which is usually caused by environmental or operational condition changes. By doing so, the variation of SHM algorithms can be identified and the threshold level for damage identification can be established. Figure 7 shows the history of the impedance variation over slight temperature fluctuation. Only 5 PZT patches (PZTs 1, 3, 5, 7, 9) were used for impedance measurement. As can be seen in Figure 7, the impedance is dependent on temperature. For a temperature variation of 1.5 degrees centigrade, the RMSD for the impedances for the quarter-inch PZTs range from 3 to 35 and the damage indices (DIs) based on one minus the cross-correlation coefficient range from 0.002 to 0.043. Any damage index value caused by structural damage must be higher than this normal variation. When the corrosion damage was introduced between sensor 4 and 5, the a quarter-inch PZT sensors 1, 3, 5 could detect the presence of damage, and the H.O.P.S. turns the color of the sensor to red (as shown in Figure 8) suggesting that the area close to these sensors might be damaged. The RMSD damage indices are: 158 for sensor 1, 135 for sensor 3, 145 for sensor 5, and 25 for sensors 7 and 9. The DIs based on the cross-correlation coefficient are: 0.66 for sensor 1, 0.58 for sensor 3, 0.72 for sensor 5, and 0.09 for sensors 7 and 9. Both damage indices for sensors 1, 3 and 5 are well above the variation that was observed from temperature variations, but the variation in the damage indices for sensors 7 and 9 was within the normal variation. By referring the history of signature variation in the past, the users can dynamically set the threshold limit to increases the ability to detect the presence of damage.

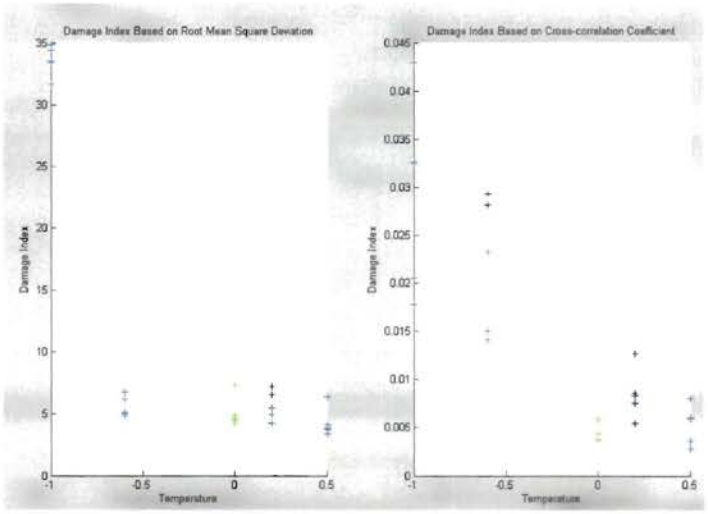

Figure 7: Changes in the Damage Indices as a Function of the Change in Temperature

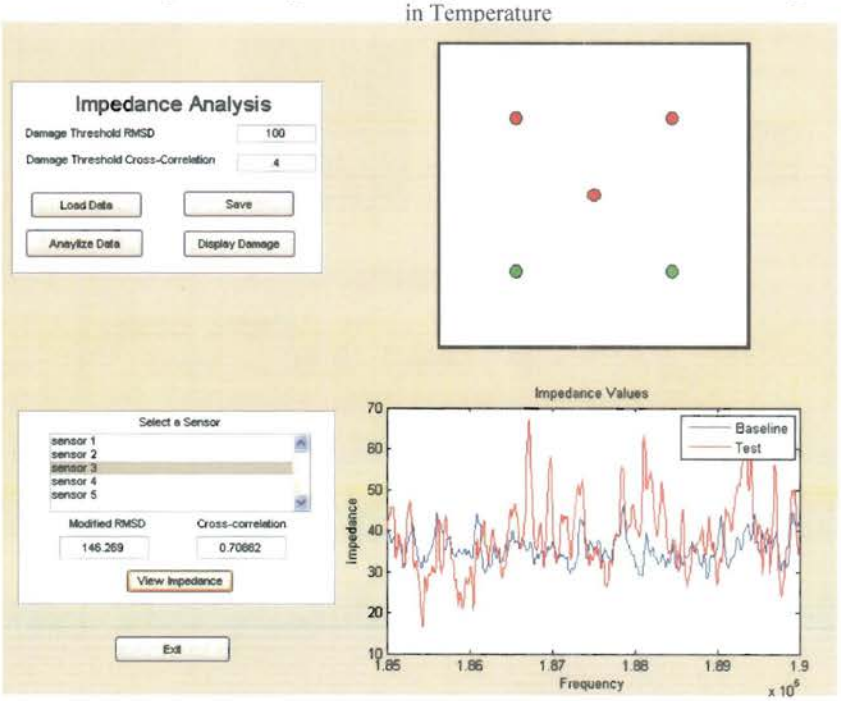

Figure 8: Impedance Analysis with Quarter-Inch PZTs for Corrosion Level 1.

5.4 Guided wave analysis

In H.O.P.S., the Wave Propagation Module displays the results of the various analysis techniques for a side-by-side comparison. Figure 9 shows the Wave Propagation Module with data for the first level of corrosion damage from the half-inch transducers. The following sections further describe the results for the various feature extraction methods.

5.4.1 Wave attenuation

As in the Impedance Module, databases of damage indices history are created for the A_0 and S_0 mode for each transducer size. The database of A_0 values for the half-inch PZTs contains damage indices ranging from 0 to 0.035. The database of DIs for the A_0 wave for the quarter-inch PZTs contains values that range from 0 to 0.012. The database of S_0 values for the half-inch PZTs contains damage indices ranging from 0 to 0.043. The database of S_0 values for the quarter-inch PZTs contains damage indices ranging from 0 to 0.043. The damage indices for the quarter-inch PZTs show less variation from test to test.

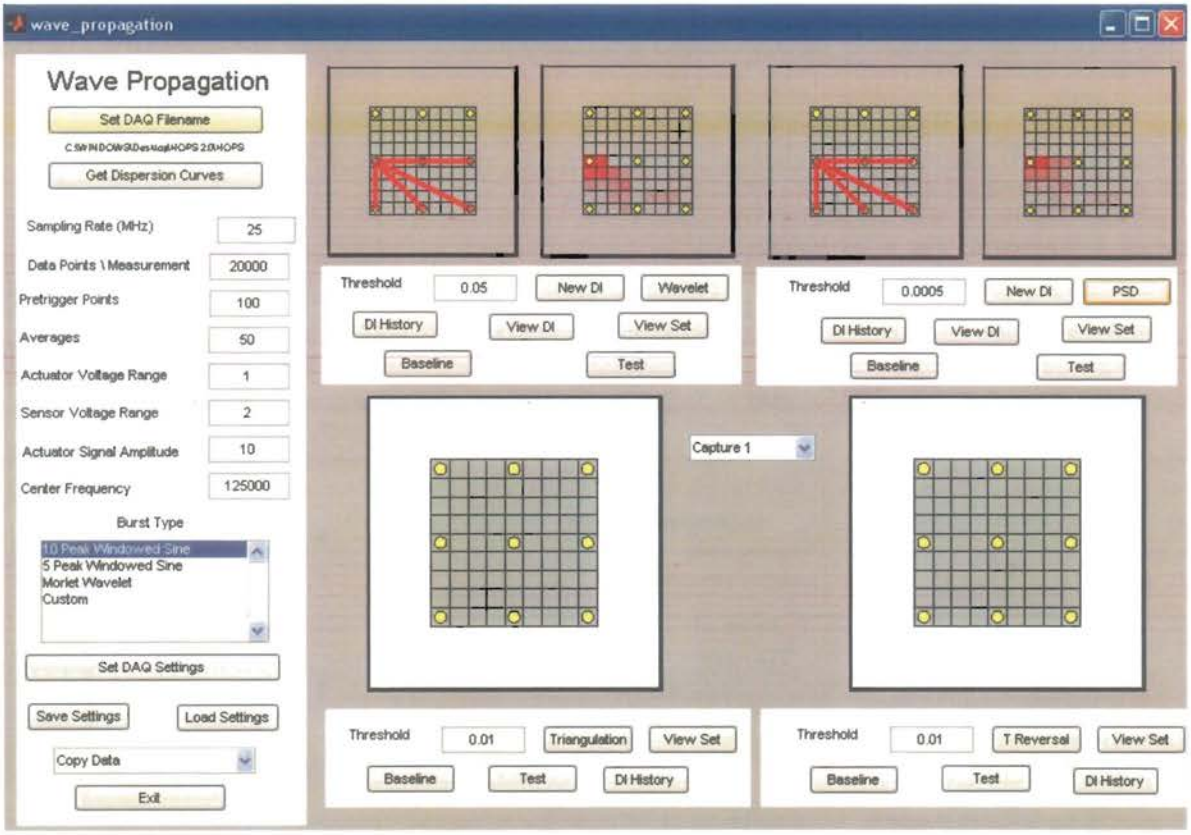

Figure 9: Wave Propagation Module with Data for Level One Corrosion from the Half-Inch Transducers.

Putty is placed between sensors five and eight. The A_0 and S_0 modes are utilized and compared for the various sensor sizes. The S_0 waves for both transducer sizes were insensitive to the putty. Figure 10 shows the damaged paths and the corresponding damage grid.

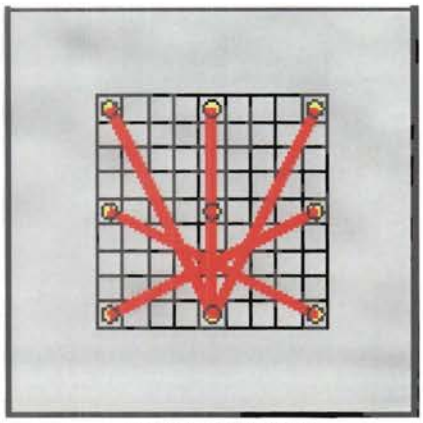

(a) Damaged Paths

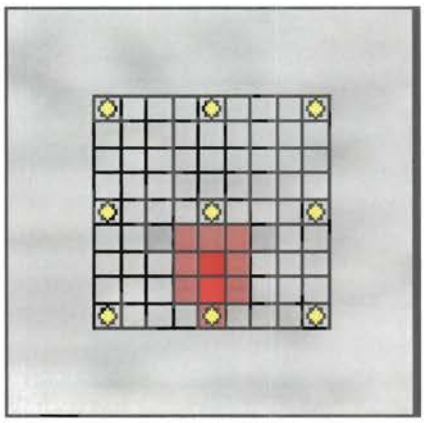

(b) Damage Grid

Figure 10: Location of Damage for Simulated Damage from A_0 waves.

A one inch diameter circle of corrosion is then introduced between sensors 4 and 5. Two steps of corrosion are introduced. The first level of corrosion is 0.56 mm (0.022 inches) deep. The second level of corrosion is 0.86 mm (0.034 inches) deep. For corrosion damage, the A_0 and S_0 modes are utilized. For the half-inch PZT transducers, both the modes place the damage within 3 inches of the actual location for both damage levels. For the quarter-inch PZT transducers, both modes place the damage within 6 inches of the actual location. Figure 11 shows how the damage indices of the damaged paths compare to those of the database and the undamaged paths for the S_0 mode for damage level one. The damage indices from the test data is shown in red, while the database values are displayed in blue. Figure 12 shows the damaged paths in red and the corresponding damaged area. The half-inch PZT transducers give the best results for identifying the location of damage.

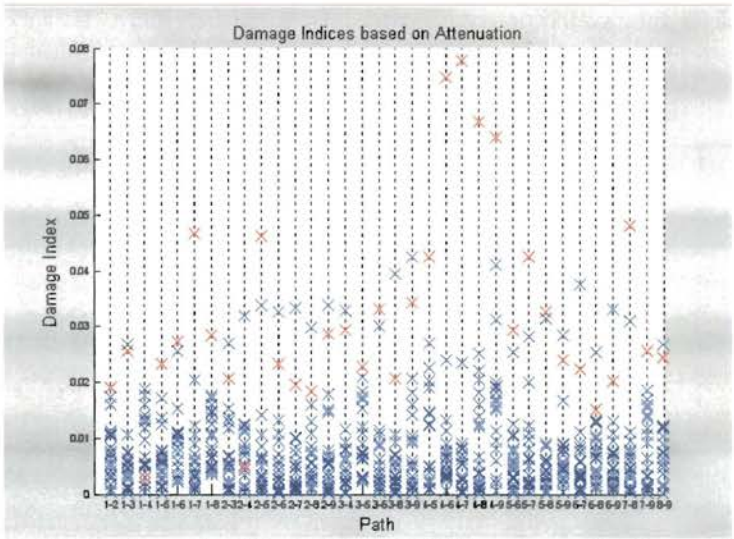

Figure 11: DIs for S_0 mode of the Half-Inch PZT Transducers for Damage Level 1.

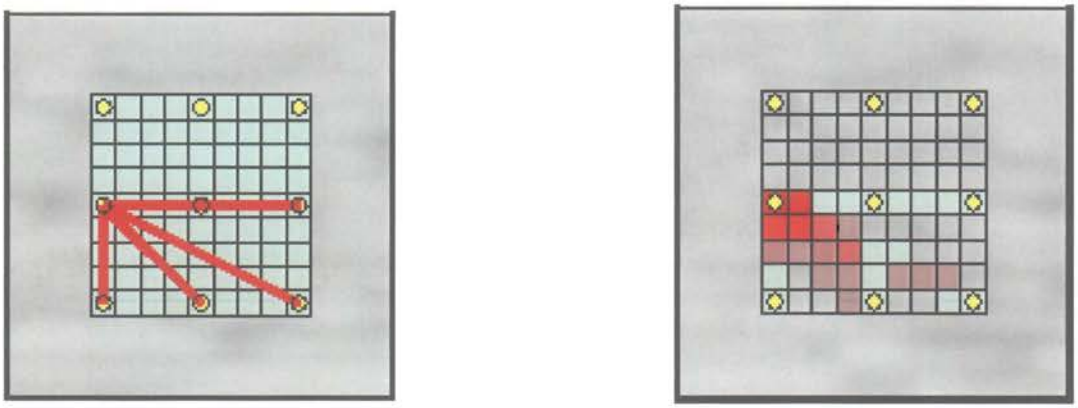

(a) Damage Paths (b) Damage Grid

Figure 12: Location of Damage for S_0 mode of the Half-Inch PZT Transducers for Damage Level **1**.

5.4.2 Guided wave power spectral density

Databases of damage indices are collected for the A_0 and S_0 modes for both quarter and half-inch PZTs. The damage indices for the A_0 mode for the half-inch PZTs range from 0 to $1.25*10^{-3}$. For the quarter-inch PZTs the damage indices range from 0 to $8.1*10^{-6}$. The damage indices for S_0 mode for the half-inch PZTs range from 0 to $8.5*10^{-5}$. For the quarter-inch PZTs the damage indices range from 0 to $1.5*10^{-4}$.

For the simulated damage where putty is placed between sensors 5 and 8, the A_0 and S_0 modes are utilized and compared for the different sensor sizes. As with the wave attenuation, the S_0 mode was insensitive to the putty for both sensor sizes. The data collected using both the quarter-inch and half-inch PZTs leads to the proper identification of the location of the damage. Information from the quarter-inch transducers allows for a more precise location of the damage (Figure 13).

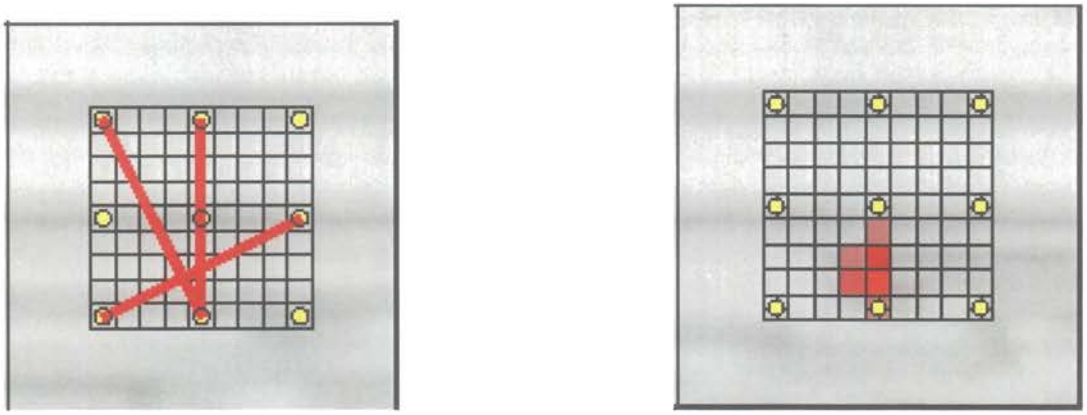

(a) Damaged Paths (b) Damage Grid

Figure 13: Location of Damage for Simulated Damage from A_0 waves.

For corrosion damage, the A_0 and S_0 modes are utilized. The A_0 mode for the half-inch PZTs locates the damage within 3 inches of the actual location for damage level one. The S_0 mode for both size transducers locates the damage within 3 inches of the actual location damage for both levels one and two. Figure 14 shows how the damage indices of the damaged paths compare to those of the database and the undamaged paths for the S_0 mode for damage level one. Figure 15 shows the damaged paths and the corresponding damage grid. The half-inch PZTs yield better results for the damage indices based on the power spectral density.

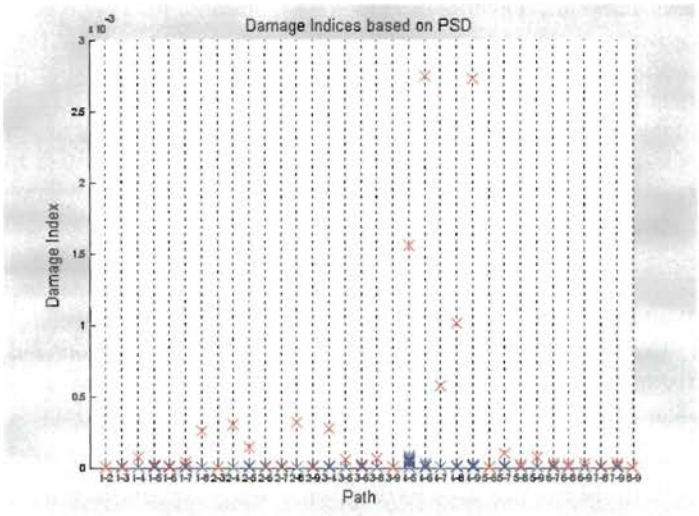

Figure 14: DIs for the S_0 mode of the Half-Inch PZTs for Damage Level One.

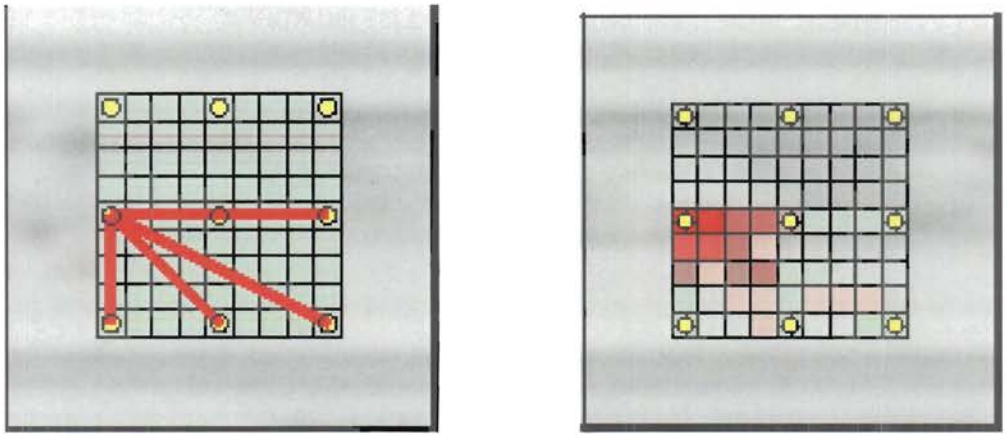

(a) Damaged Paths (b) Damage Grid

Figure 15: Location of Damage for S_0 mode of the Half-Inch PZTs for Damage Level One.

6. CONCLUSIONS

Specific topics that have not been extensively addressed in the SHM literature are i) the development of user friendly and automated software for data analysis; ii) coupling the sensing hardware directly with SHM data interrogation software. This work is trying to address these issues, and the successful studies toward these areas will help to transition the current state-of-the-art of SHM to full-scale industrial adoption. By integrating various data interrogation and signal processing algorithms, a powerful SHM tool has been developed that can be applied to a wide variety of applications. Each algorithm produces various levels of efficacy based on the type of damage present and the mode of wave utilized in gathering data. In some cases one method will detect the presence of damage, and another can determine the location or the severity of damage. For example, the analyst could perform an impedance test to determine if damage is present in the structure. Then, the analyst could estimate if the damage is in the structure or the sensors themselves. If the analyst determines that damage is present, wave propagation could then be used to locate the damage. Including the ability to compile a database of baseline values, allows the analyst the ability to determine if changes detected by the SHM algorithms are statistically significant and thus are due to damage and not the normal changes caused environmental conditions. By integrating the different techniques for interrogating the structure and then extracting the features, the analyst can efficiently test for and identify damage within a structure.

Future work is required to realize the full potential of H.O.P.S.. Currently, the H.O.P.S. software is configured to run only on a specific type of hardware. It would be beneficial to reconfigure it to be more flexible and run on a variety of platforms. In additon, several newly developed active-sensing damage identification techniques will be implemented including those utilizing reflection features and nonlinear acoustics in guided waves. Furthermore, to fully realize the potential of the integrated algorithm scheme assembled in H.O.P.S., it is necessary to optimize the SHM algorithms and sensor/actuator deploy for a variety of materials, configurations, and damage types that would result in flexible, easy to use tool for SHM in many types of structures and these works are currently undertaken by authors.

REFERENCES

[1] Park, G., Sohn, H., Farrar, C.R., Inman, D.J. "Overview of Piezoelectric Impedance-Based Health Monitoring and Path Forward," *The Shock and Vibration Digest*, **35**, 451-463 (2003).

[2] Park, G., Farrar, C.R., Lanza di Scalea, F., Coccia, S. "Performance Assessment and Validation of Piezoelectric Active-Sensors in Structural Health Monitoring," *Smart Materials and Structures* (2006).

[3] Wait, J.R., Park, G., Farrar, C.R. (2004). Integrated Structural Health Assessment using Piezoelectric Active Sensors, Shock and Vibration, **12**, 389-405 (2004).

[4] Raghavan, A., & Cesnik, C.E.S. (2004) Modeling of piezoelectric-based Lamb-wave generation and sensing for structural health monitoring. *Proceedings of SPIE,* v. 5391, Bellingham, VA 419-430 (2004).

[5] Park, G., Farrar, C.R., Rutherford, A.C., & Roberstson, A.N. "Piezoelectric Active Sensor Self-Diagnostics using Electrical Admittance Measurements," *ASME Journal of Vibration and Acoustics*, **128**, 469-476 (2006).

[6] Lee, B.C. & Staszewski, W.J. (2003) Modeling of Lamb Waves for Damage Detection in Metallic Structures: Part I. Wave Propagation. *Smart Materials and Structures*, **12** (5), 804-814.

[7] Kessler, S.S., Spearing, S.M., & Soiutis, C. "Structural Health Monitoring in Composite Materials Using Lamb Wave Methods," *Smart Materials and Structures*, **11**, 269-278 (2002).

[8] Abbate, A., Koay, J., Frankel, J., Schroefer, S.C., & Das, P. "Signal Detection and Noise Suppression Using a Wavelet Transform Signal Processor: Applications to Ultrasonic Flaw Detection," IEEE *Transactions on Ultrasonics, Ferroelectrics, and Frequency Control*, **44**, pp. 14-26, (1997).

[9] Sohn, H., Park, G., Wait, J.R., Limback, N.P., & Farrar, C.R. "Wavelet-Based Active Sensing for Delamination Detection in Composite Structures," *Smart Materials and Structures*, **13** (1), 153-160 (2004).

[10] Lind, R., Kyle, S., & Brenner, M. "Wavelet Analysis to Characterize the Nonlinearities and Predict Limit Cycles of an Aeroelastic System," *AIAA/ASME/ASCE/AHS/ASC Structures, Structural Dynamics & Materials Conference*, **2**, 337-356 (2001).

[11] Park, G., Kabeya, K., Cudney, H.H., & Inman, D.J. "Impedance-Based Structural Health Monitoring for Temperature Varying Applications," *JSME International Journal*, **42** (2), 249-258 (1999).

[12] Swartz, R.A., Flynn, E., Backman, D., Hundhausen, R.J., & Park, G. "Active Piezoelectric Sensing for Damage Identification in Honeycomb Aluminum Panels," *Proceedings of 24th International Modal Analysis Conference*, Jan 30- Feb 2, St Louis, MO (2006).

[13] V. Giurgiutiu, A. Zagrai, J.J. Bao, "Damage Identification in Aging Aircraft Structures with Piezoelectric Wafer Active Sensors," *Journal of Intelligent Material Systems and Structures*, **15**, 673-688 (2004).

[14] S. Bhalla, C.K. Soh, "Structural Impedance-based Damage Diagnosis by Piezo-Transducers," *Earthquake Engineering & Structural Dynamics*, **32**, 1897-1916 (2003).

[15] Park, G., Farrar, C.R., Lanza di Scalea, F., Coccia, S., "Performance Assessment and Validation of Piezoelectric Active Sensors in Structural Health Monitoring," *Smart Materials and Structures*, **15**(6), 1673-1683 (2006).